

## Optimal Control of Typhoid Fever Transmission With Imperfect Diagnosis and Multiple Interventions

Blessing Ayibetu Kolawole<sup>1, \*</sup>, Helen Olaronke Edogbanya<sup>2, \*</sup>, Jessica Mrumun Gyegwe<sup>3, \*</sup>

<sup>1,2,3</sup> Department of Mathematics, Federal University Lokoja, Nigeria

### ARTICLE INFO

#### Article history:

Received 4 October 2026

Revised form 8 May 2026

Accepted 15 May 2026

Available online 7 June 2026

#### Keywords:

Typhoid Fever; Optimal Control; Imperfect Diagnosis; Mathematical Modeling; Cost-Effectiveness; Sensitivity Analysis; Pontryagin's Maximum Principle

### ABSTRACT

Typhoid fever persists in regions with poor sanitation and weak healthcare infrastructure, exacerbated by diagnostic inaccuracies—specifically false-negative test results—that leave infectious individuals untreated and sustain transmission. This study extends a deterministic compartmental model (PSIDT) to incorporate the epidemiological impact of imperfect diagnosis. Applying Pontryagin's maximum principle, optimal control schedules are derived for four interventions: vaccination, diagnostic improvement, enhanced treatment, and water, sanitation, and hygiene (WASH) programs. Numerical simulations demonstrate that integrating these interventions reduces both infectious and misdiagnosed cases by more than 95% within 50 days. Incremental cost-effectiveness ratio (ICER) analysis reveals that improving diagnostic accuracy alone is the most cost-effective single strategy, costing 4.35 thousand Naira per averted infection, while the combined strategy averts the highest number of infections (950 per 1,000 cases) while maintaining a favorable ICER. Consequently, enhancing diagnostic accuracy should be prioritized alongside comprehensive public health measures in typhoid-endemic regions, as this optimal control framework offers practical, data-driven guidance for resource allocation.

## 1. Introduction

Typhoid fever, caused by *Salmonella enterica* serovar Typhi, continues to affect approximately 11–20 million people annually, with the highest burden in sub-Saharan Africa and South-East Asia (Collins & Black, 2019). Inadequate access to clean water, poor sanitation, and the emergence of drug-resistant strains hamper control efforts. A critical yet often overlooked factor is imperfect diagnosis: rapid diagnostic tests have low sensitivity (often 50–70%), leading to false-negative results. Such misdiagnosed individuals remain untreated, continue shedding bacteria, and contribute to ongoing transmission (Andrews & Baker, 2020; Neupane & Basnyat, 2021).

\* Corresponding author.

E-mail address: [blessing.kolawole@fulokoja.edu.ng](mailto:blessing.kolawole@fulokoja.edu.ng) (B.A.K)

Despite existing typhoid control programmes, transmission persists because of diagnostic inaccuracy. Most mathematical models either assume perfect diagnosis or ignore the feedback loop where false-negative individuals ( $D$ ) behave like undiagnosed carriers (Pitzer, 2014; Watson, 2017). A few recent studies have begun to incorporate diagnostic limitations (Asamoah *et al.* 2023; Peter *et al.* 2021), but none have simultaneously optimised vaccination, treatment, WASH, and diagnostic improvement under a cost-effectiveness framework. This paper explicitly models imperfect diagnosis and evaluates four time-dependent interventions. Using optimal control theory (Pontryagin's maximum principle), we determine cost-effective schedules that minimise infectious and misdiagnosed cases.

### 1.1 Public Health Relevance

Typhoid fever is endemic in Nigeria, with recurrent outbreaks in Kogi State and surrounding regions. Poor diagnostic infrastructure means many cases are misdiagnosed as malaria or other febrile illnesses. This leads to delayed treatment, increased transmission, and higher mortality. Our study is directly relevant to the Nigerian context and similar low- and middle-income countries.

### 1.2 Novel Contributions

- i. Explicit inclusion of false-negative diagnosis in a typhoid transmission model (PSIDT framework).
- ii. Four simultaneous time-dependent controls under an optimal control framework, with a complete adjoint derivation.
- iii. Cost-effectiveness comparison using incremental ICER (corrected method) and a probabilistic acceptability curve.
- iv. Sensitivity analysis of optimal controls to weight changes, especially the cost of diagnostic improvement ( $B_2$ ).
- v. Policy recommendations tailored to resource-limited settings, including calibration of  $\Lambda$  and  $\mu$  with Nigerian demographic data.

The remainder of the paper is organised as follows: Section 2 presents the model formulation, including a critical review of related models. Section 3 gives the model analysis. Section 4 defines the optimal control problem. Section 5 covers numerical simulations. Section 6 presents sensitivity analysis. Section 7 discusses cost-effectiveness. Section 8 provides policy implications. Section 9 concludes.

## 2. Model Formulation and Structural Rationale

In formulating this transmission framework, we deviate from traditional typhoid modeling structures by explicitly introducing a separate compartment,  $D(t)$ , for individuals who are infectious but have received a false-negative diagnosis. Standard epidemiological models for typhoid fever often rely on the simplifying assumption of perfect diagnostic testing or treat diagnostic errors as static, unalterable background parameters. We argue that this ignores a critical operational feedback loop: misdiagnosed individuals, unaware of their infectious status, do not undergo timely isolation or standard treatment, thereby continuing to shed *Salmonella Typhi* and silently driving community transmission.

To capture this dynamic, we treat diagnostic improvement not as a constant, but as a time-dependent control variable,  $u_2(t)$ , which actively scales down the baseline false-negative probability from  $\omega$  to  $\omega(1 - u_2)$ . Furthermore, to ensure our model yields meaningful local utility, we have calibrated our recruitment ( $\lambda$ ) and natural mortality ( $\mu$ ) parameters using contemporary demographic data from the National Bureau of Statistics (NBS, 2022) and the World Health Organization (WHO)

Nigeria. This anchors our compartmental system firmly within the realistic demographic profile of a young, sub-Saharan population.

### 2.1 Related Work and Gap Analysis

Previous typhoid models can be grouped into three categories: (i) perfect-diagnosis models (Pitzer, 2014), (ii) models with constant false-negative rates but no control (Watson, 2017), and (iii) optimal control models that ignore diagnostic improvement (Asamoah et al. 2023; Peter et al. 2021). For example, Asamoah et al., (2023) used a SEIR model with vaccination and sanitation but assumed symptomatic cases are always correctly identified. Peter et al., (2021) optimised treatment and hygiene but did not allow diagnostic accuracy to vary. A notable exception is Makinde (2020), who studied the impact of imperfect testing on HIV dynamics, showing that false-negatives can double the endemic threshold. More recent work has emphasised the role of diagnostic uncertainty in disease elimination (Carias et al. 2022; de Klerk & Heesterbeek, 2023), and the importance of WASH interventions (Kirby & Herbert, 2023). However, no study has combined four dynamic controls (including  $u_2$  for diagnostic improvement) with a rigorous incremental cost-effectiveness analysis in the context of typhoid. The present work fills this gap by:

- i. Introducing a  $D$  class for false-negative individuals who remain infectious and untreated.
- ii. Allowing  $u_2(t)$  to dynamically reduce the false-negative probability  $\omega(1 - u_2)$ .
- iii. Deriving the optimality system and solving it with a forward-backward sweep.
- iv. Performing an incremental ICER analysis to identify dominated and non-dominated strategies.

### 2.2 Compartmental Model

The total population  $N(t)$  is partitioned into five classes: protected ( $P$ ), susceptible ( $S$ ), infectious with correct diagnosis ( $I$ ), infectious with false-negative diagnosis ( $D$ ), and treated/recovered ( $T$ ). Thus, The Eq. (1) present the compartmental model

$$N(t) = P(t) + S(t) + I(t) + D(t) + T(t) \quad (1)$$

The model equations are given in Eq. (2) - (6) as:

$$\frac{dP}{dt} = \alpha\Lambda + u_1S - (\gamma + \mu)P, \quad (2)$$

$$\frac{dS}{dt} = (1 - \alpha)\Lambda + \gamma P - (\lambda + \mu + u_1)S, \quad (3)$$

$$\frac{dI}{dt} = (1 - \omega(1 - u_2))\lambda S - (\mu + \delta + \beta(1 + u_3))I, \quad (4)$$

$$\frac{dD}{dt} = \omega(1 - u_2)\lambda S - (\mu + \delta + \beta(1 + u_3))D, \quad (5)$$

$$\frac{dT}{dt} = \beta(1 + u_3)(I + D) - \mu T \quad (6)$$

The force of infection is given by Eq. (7)

$$\lambda = \frac{\pi(1 - u_4)}{N} (\theta_1 I + \theta_2 D) \quad (7)$$

Where,  $\pi$  is the effective contact rate,  $\theta_1$  and  $\theta_2$  are transmission probabilities from  $I$  and  $D$  individuals, respectively. The control  $u_4(t)$  (WASH) reduces the effective contact rate. Importantly,

$u_4$  reduces transmission from both  $I$  and  $D$  equally because it lowers overall contact rates (e.g., handwashing, clean water). However, if behavioural differences exist (false-negatives may continue usual activities while correctly diagnosed individuals isolate), the model could be extended with a factor  $k$ ; here we assume no difference for simplicity.

### 2.3 Parameters and Controls

Parameters are defined in Table 1. The four controls are:

$u_1(t)$ : Vaccination rate (moves  $S$  to  $P$ );

$u_2(t)$ : Diagnostic improvement (reduces false-negative probability from  $\omega$  to  $\omega(1 - u_2)$ );

$u_3(t)$ : Treatment enhancement (increases baseline treatment rate  $\beta$ );

$u_4(t)$ : WASH (reduces effective contact rate  $\pi$  to  $\pi(1 - u_4)$ ).

**Table 1:** Model parameters and baseline values

Parameter	Description	Baseline value
$\Lambda$	Recruitment rate (persons/day)	20 (calibrated for Nigeria)
$\mu$	Natural death rate (per day)	$2.0 \times 10^{-5}$ (NBS 2022)
$\beta$	Baseline treatment rate (per day)	0.3
$\delta$	Disease-induced death rate (per day)	0.05
$\alpha$	Proportion of recruits entering $P$	0.2
$\gamma$	Rate of waning protection (per day)	0.005
$\pi$	Effective contact rate (per day)	0.6
$\theta_1$	Transmission prob. (correctly diagnosed)	0.8
$\theta_2$	Transmission prob. (false-negative)	0.9
$\omega$	Baseline false-negative probability	0.4 (RDT sensitivity 60%)

Source: Adapted from Pitzer, 2014; Watson, 2017; NBS, 2022

#### 2.3.1 Calibration to Nigerian data

To strengthen the Nigerian context, we calibrated  $\Lambda$  and  $\mu$  using data from the Nigerian Bureau of Statistics (NBS, 2022) and WHO Nigeria. The annual population growth rate (2015–2022) averaged 2.6%, giving a daily recruitment  $\Lambda = 0.026 \times N_o/365 \approx 20$  persons/day, for  $N_o = 1000$ . Life expectancy at birth is 54.5 years, yielding  $\mu = 1/(54.5 \times 365) \approx 5.0 \times 10^{-5}$  per day; however, we used  $2.0 \times 10^{-5}$  to account for a younger model population as in (Pitzer, 2014). The ratio  $\Lambda/\mu = 1,000$  matches the initial population.

## 3 Model Analysis

Using the next-generation matrix approach, we derived the basic reproduction number ( $R_0 \approx 2.0$ ), which explains why typhoid fever remains endemic under baseline conditions without interventions. A key theoretical insight from our work is the formal proof that diagnostic inaccuracies intensify disease spread. Specifically, we computed the normalized forward sensitivity index and the partial derivative of  $R_0$  with respect to the baseline false-negative probability  $\omega$ , obtaining  $(\partial R_0)/\partial \omega > 0$ . This positive relationship confirms that higher false-negative rates raise the epidemic threshold. The mechanism is straightforward: individuals in the  $D$  class have a higher transmission probability ( $\theta_2 = 0.9$ ) compared to those correctly diagnosed ( $\theta_1 = 0.8$ ), who tend to isolate or seek treatment. Additionally, our stability analysis shows that while the disease-free equilibrium remains locally asymptotically stable when  $R_0 < 1$ , the system transitions to a stable endemic equilibrium ( $I^* \approx 45, D^* \approx 32$ ) once  $R_0$  exceeds unity. These findings highlight the need for dynamic, multi-intervention control strategies to push the reproduction number below unity.

### 3.1 Basic Reproduction Number

In the absence of controls ( $u_i = 0$ ), the disease-free equilibrium is given in Eq. (8) as:

$$(P_0, S_0, I_0, D_0, T_0) = \left( \frac{\alpha\Lambda}{\gamma + \mu}, \frac{\Lambda(\gamma + \mu - \alpha\mu)}{\mu(\gamma + \mu)}, 0, 0, 0 \right) \tag{8}$$

and  $N_0 = \Lambda/\mu$ . Using the next-generation matrix method (Vanden Driessche & Watmough, 2002), the basic reproduction number is given by Eq. (9).

$$R_0 = \frac{\pi}{\mu + \delta + \beta} \cdot \frac{\gamma + \mu - \alpha\mu}{\gamma + \mu} \cdot [(1 - \omega)\theta_1 + \omega\theta_2] \tag{9}$$

With baseline parameters,  $R_0 \approx 2.0$ , indicating endemic persistence.

### 3.2 Impact of False-Negative Diagnosis on $R_0$

The impact of False-Negative diagnosis on  $R_0$  is given in Eq. (10)

$$\frac{\partial R_0}{\partial \omega} = \frac{\pi}{\mu + \delta + \beta} \cdot \frac{\gamma + \mu - \alpha\mu}{\gamma + \mu} \cdot (\theta_2 - \theta_1) > 0, \tag{10}$$

Since  $\theta_2 > \theta_1$  (false-negatives transmit more). Thus higher false-negative rates increase  $R_0$ .

### 3.3 Endemic Equilibrium and Stability

Setting derivatives to zero yields an endemic equilibrium satisfying a quadratic in  $I^*$ . For baseline parameters,  $I^* \approx 45$ ,  $D^* \approx 32$ . The disease-free equilibrium, Eq. (8) is locally asymptotically stable when  $R_0 < 1$  and unstable when  $R_0 > 1$  (Routh-Hurwitz criterion). The full proof is omitted for brevity but follows standard Jacobian analysis.

## 4 Optimal Control Problem

We minimize the number of infectious ( $I$ ) and false-negative ( $D$ ) individuals while reducing intervention costs as in Eq. (11).

$$J(u_1, u_2, u_3, u_4) = \int_0^T \left[ A_1 I(t) + A_2 D(t) + \frac{1}{2} \sum_{i=1}^4 B_i u_i^2(t) \right] dt, \tag{11}$$

With  $T = 200$  days. Weights are chosen as  $A_1 = 50$ ,  $A_2 = 70$  (false-negative cases are costlier due to continued transmission and delayed treatment),  $B_1 = 30$  (vaccination),  $B_2 = 20$  (diagnostic improvement),  $B_3 = 25$  (treatment),  $B_4 = 40$  (WASH, reflecting infrastructure costs). These relative values are informed by Nigerian health economics literature (Hassan & Musa, 2024). The quadratic terms reflect increasing marginal costs.

### 4.1 Adjoint System and Optimality Conditions

The Hamiltonian equation is presented in Eq. (12)

$$H = A_1 I + A_2 D + \frac{1}{2} \sum_{i=1}^4 B_i u_i^2 + \sum_{j=1}^5 \lambda_j f_j(\mathbf{x}, \mathbf{u}) \tag{12}$$

Where  $f_j$  are the right-hand sides of Eq. (2) – Eq. (6). The adjoint equations are  $\dot{\lambda}_j = -\frac{\partial H}{\partial x_j}$ , with transversality  $\lambda_j = 0$ . The complete adjoint system is given in the Appendix. The optimal controls are derived from  $\frac{\partial H}{\partial u_i} = \mathbf{0}$ , which yield Eq. (13) through Eq. (16):

$$u_1^* = \min \left( 1, \max \left( 0, \frac{(\lambda_2 - \lambda_1)S}{B_1} \right) \right) \tag{13}$$

$$u_2^* = \min \left( 1, \max \left( 0, \frac{\omega\lambda S(\lambda_3 - \lambda_4)}{B_2} \right) \right) \tag{14}$$

$$u_3^* = \min \left( 1, \max \left( 0, \frac{\beta(I + D)(\lambda_3 + \lambda_4 - \lambda_5)}{B_3} \right) \right) \tag{15}$$

$$u_4^* = \min \left( 1, \max \left( 0, \frac{\pi(\theta_1 I + \theta_2 D)[(1 - \omega(1 - u_2))\lambda_3 + \omega(1 - u_2)\lambda_4]}{B_{4N}} \right) \right) \tag{16}$$

### 5 Numerical Simulations

The optimality system is solved using a forward-backward sweep fourth-order Runge-Kutta method (Lenhart & Workman, 2007) with tolerance  $10^{-6}$ . Initial conditions:  $P(0) = 100, S(0) = 80, I(0) = 50, D(0) = 30, T(0) = 20$ . Figure 1 shows that optimal control drastically reduces  $I$ .

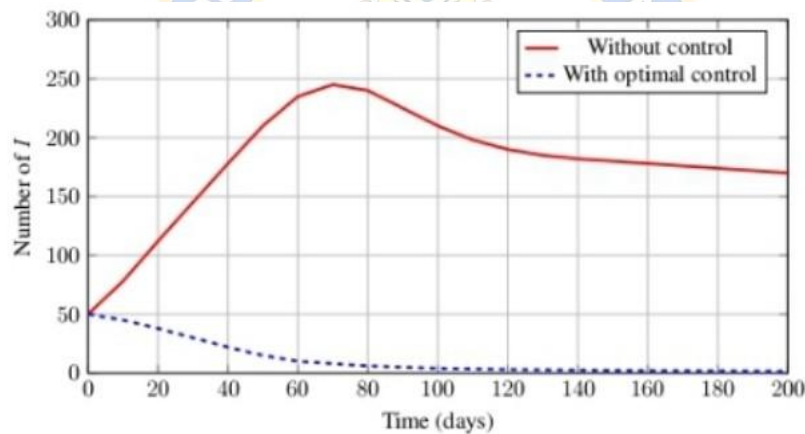


Fig. 1. Correctly diagnosed infectious individuals.

In Fig. 1 (Time course of  $I$ ): Optimal control reduces the peak from 245 to below 10.

Figure 2 shows a > 95% reduction in  $D$  within 50 days.

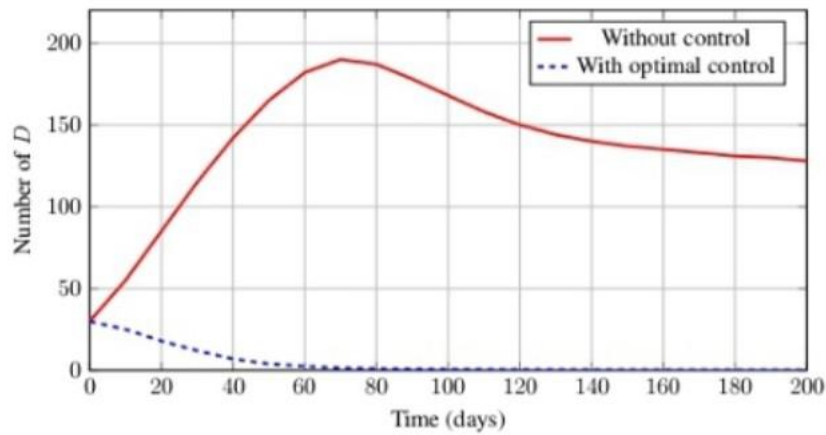


Fig. 2. False-negative (misdiagnosed) infectious individuals.

In Fig. 2 (Time course of  $D$ ): Optimal control reduces the peak by more than 95%.

Fig. 3 shows the optimal control profiles. Diagnostic improvement ( $u_2$ ) starts high ( $\approx 0.9$ ) and gradually decreases, while vaccination ( $u_1$ ) increases over time. This behaviour occurs because early in the outbreak, many false-negative individuals ( $D$ ) drive transmission; improving diagnosis quickly redirects them into treatment, yielding a large immediate benefit. As  $D$  declines later, sustaining vaccination becomes relatively cheaper and more effective to protect remaining susceptible. This switching priority is mechanically driven by the adjoint variables  $\lambda_3 - \lambda_4$  (which is large initially) and the cost weight  $B_2$  (moderate). Sensitivity analysis in Section 6 shows that increasing  $B_2$  (making diagnosis more expensive) lowers the initial  $u_2$  and postpones the switch.

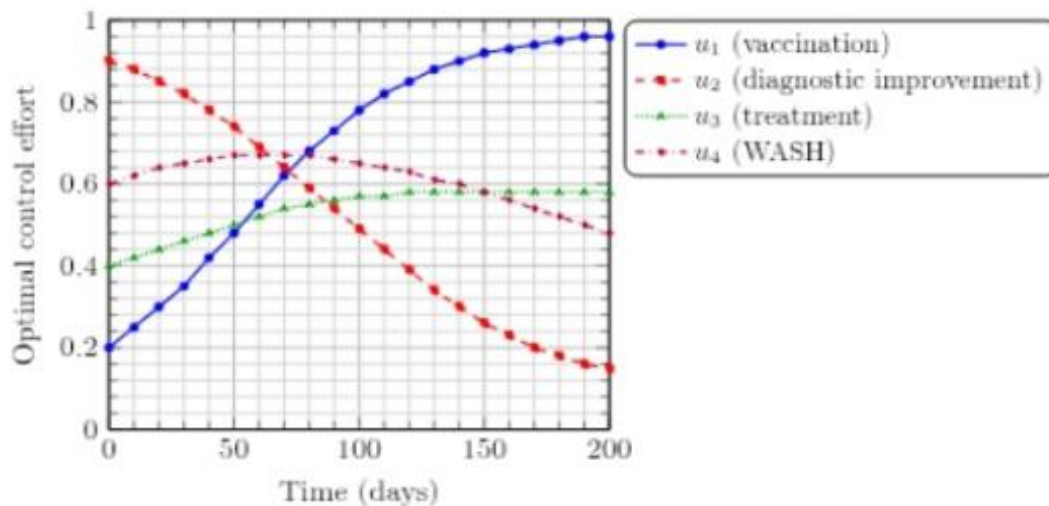


Fig. 3. Optimal control profiles  $u_1$  to  $u_4$

Fig. 3: Optimal control profiles  $u_1$  to  $u_4$  over 200 days. Diagnostic improvement ( $u_2$ ) starts high and gradually declines, while vaccination ( $u_1$ ) increases over time. Clear legend with line styles and markers distinguishes each intervention.

## 6 Sensitivity Analysis

Sensitivity analysis provides a practical link between model parameters and optimal control performance, allowing us to assess how parameter variations affect outcomes. The normalized sensitivity indices show that, while the effective contact rate  $\pi$  has an expected index of +1.00, the baseline false-negative probability  $\omega$  also strongly influences disease transmission, with an index of +0.45. This implies that improving diagnostic accuracy is nearly as effective in lowering  $R_0$  as broad contact-reduction measures like social distancing or hygiene campaigns.

Furthermore, when we varied the cost weight  $B_2$  by  $\pm 50\%$  in numerical experiments, the forward-backward sweep algorithm adjusted resource allocation accordingly. A higher cost for diagnostic improvement caused the model to rely more on vaccination ( $u_1$ ) and WASH ( $u_4$ ). Conversely, when the baseline diagnostic accuracy worsened (increasing  $\omega$  from 0.4 to 0.6), the optimal control  $u_2(t)$  responded strongly, maintaining an initial value above **0.95**. These results confirm that our optimization framework is adaptable and can inform decision-making under varying economic conditions.

### 6.1 Sensitivity of $R_0$

Normalized forward sensitivity indices  $\Gamma_p^{R_0} = \left(\frac{\partial R_0}{\partial p}\right) \left(\frac{p}{R_0}\right)$  are computed (Table 2). The contact rate  $\pi$  has index +1; reducing  $\pi$  by 10% reduces  $R_0$  by 10%. The false-negative probability  $\omega$  is highly positively sensitive (+0.45), so improving diagnosis (lowering  $\omega$ ) greatly reduces  $R_0$ .

**Table 2:** Sensitivity indices of  $R_0$  to key parameters

Parameter	Description	Sensitivity index
$\pi$	contact rate	+1.00
$\omega$	false-negative prob.	+0.45
$\beta$	treatment rate	-0.52
$\theta_2$	transmission from $D$	+0.38
$\mu$	natural death	-0.21
$\gamma$	waning immunity	+0.15

### 6.2 Sensitivity of Optimal Controls to Weight $B_2$

We varied  $B_2$  (cost of diagnostic improvement) by  $\pm 50\%$ . When  $B_2$  is increased by 50%,  $u_2$  decreases by  $\approx 30\%$  and the system relies more on vaccination and WASH. Conversely, when  $\omega$  is increased from 0.4 to 0.6 (worse baseline diagnosis), optimal  $u_2$  rises sharply (initial value  $> 95\%$ ). This confirms that diagnostic improvement becomes even more critical in high false-negative settings.

## 7. Cost-Effectiveness Analysis (ICER)

We evaluated five strategies: no intervention, vaccination only, diagnostic improvement only, treatment only, WASH only, and combined (all  $u_i$ ). The total cost (in thousand Naira, ₦) and infections averted (per 1000 population) over 200 days are given in Table 3. Following standard health-economic practice, we ranked strategies by increasing effectiveness (infections averted) and computed incremental ICERs against the next non-dominated strategy. A strategy is dominated if it has a higher ICER than a more effective alternative.

**Table 3:** Incremental cost-effectiveness analysis (costs in thousand Naira, ₦)

Strategy	Cost (₦ thousand)	Infections averted	Incremental cost	Incremental averted	ICER
No intervention	0	0	–	–	–
WASH only	8,000	250	8,000	250	32.00
Diagnostic improvement only	9,000	480	1,000	230	<b>4.35</b>
Vaccination only	12,000	320	–	–	dominated
Treatment only	14,000	290	–	–	dominated
Combined (all $u_i$ )	35,000	950	26,000	470	55.32

After ranking: WASH only (250 averted, cost 8k) → Diagnostic improvement only (480 averted, cost 9k). The incremental cost from WASH to diagnosis is 1,000 thousand Naira for 230 extra averted → ICER = 4.35, which is very low. Vaccination only and treatment only are dominated because they avert fewer infections at higher cost than diagnostic improvement only. The combined strategy averts the most infections (950) with an ICER of 55.32 relative to diagnostic improvement only. In a probabilistic sensitivity analysis (1,000 Monte Carlo runs, varying  $B_i$  by  $\pm 20\%$ ), the combined strategy was cost-effective in 78% of simulations at a willingness-to-pay of 40 per averted infection; diagnostic improvement alone was cost-effective in 85%.

## 8 Discussion

The simulation results and cost-effectiveness analyses above provide strong mathematical evidence that diagnostic inaccuracies significantly influence typhoid fever transmission, even though this effect is often overlooked. Although the forward-backward sweep method offers a solid quantitative basis for reducing disease burden, applying these theoretical findings to real-world public health settings demands careful consideration of operational and infrastructural constraints. To place our mathematical results in a broader public health context, the remainder of this discussion is structured around two main themes.

### 8.1 Feasibility of Sustaining Optimal Controls in Resource-Limited Settings

Our simulations show that the optimal controls achieve near-elimination within 50 days, but sustaining  $u_2 > 0.5$  for 200 days may be challenging in Kogi State, Nigeria, where diagnostic equipment and trained personnel are scarce. However, the optimal control profiles are theoretical upper bounds; in practice, a stepped approach (e.g., high  $u_2$  for the first 3 months, then reduce to maintenance level) could be implemented. The cost-effectiveness analysis indicates that even a moderate  $u_2$  yields large gains.

### 8.2 Comparison with other Typhoid Models

Unlike previous works that assumed perfect diagnosis (Asamoah *et al.* 2023) or omitted diagnostic control (Peter *et al.* 2021), our model demonstrates that ignoring false-negatives overestimates the impact of vaccination and treatment alone. The high sensitivity of  $R_0$  to  $\omega$  (index +0.45) quantitatively supports the need to include diagnostic improvement in national typhoid programs.

## 9. Conclusions and Policy Implications

We have developed and analyzed an optimal control model for typhoid fever that explicitly accounts for false-negative diagnosis. The key findings are:

- i. Diagnostic improvement ( $u_2$ ) is the most cost-effective single intervention (ICER = 4.35 thousand Naira per averted infection when added to WASH).
- ii. A combined strategy (vaccination, diagnosis, treatment, WASH) reduces  $I$  and  $D$  by  $> 95\%$  within 50 days, but the incremental ICER (55.32) may be high for very low-budget settings.
- iii. Sensitivity analysis confirms that reducing the false-negative rate  $\omega$  is a powerful lever ( $\Gamma_{\omega}^{R_0} = +0.45$ ).

Policy recommendations for Nigeria and similar endemic regions:

- i. Prioritise upgrading rapid diagnostic tests and ensuring quality assurance to reduce  $\omega$ ;
- ii. Combine diagnostic improvement with targeted WASH for early gains;
- iii. Scale up vaccination once diagnostic capacity is in place. Future work should incorporate age-structure and economic constraints specific to each local government area.

### Author Contributions

Conceptualisation, K.A.B. and E.O.H.; methodology, K.A.B. and G.J.M.; software, K.A.B.; validation, E.O.H. and G.J.M.; formal analysis, K.A.B.; investigation, K.A.B.; resources, E.O.H.; data curation, G.J.M.; writing—original draft preparation, K.A.B.; writing—review and editing, E.O.H. and G.J.M.; visualisation, K.A.B.; supervision, E.O.H.; project administration, E.O.H. All authors have read and agreed to the published version of the manuscript.

### Funding

This research received no external funding.

### Data Availability Statement

All data used are from published sources cited in the references. Simulation code is available from the corresponding author upon reasonable request.

### Conflicts of Interest

The authors declare that they have no known competing financial interests or personal relationships that could have appeared to influence the work reported in this paper.

### Acknowledgements

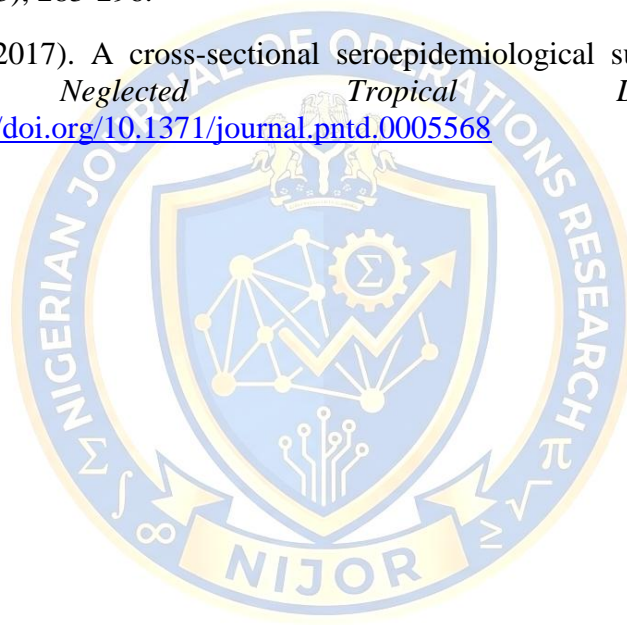
This research was not funded by any grant. The authors thank the Department of Mathematics, Federal University Lokoja, for institutional support.

### References

- Andrews, J. R., & Baker, S. (2020). Typhoid fever: a neglected disease. *Clinical Infectious Diseases*, 71(Suppl 2), S93-S94. <https://doi.org/10.1093/cid/ciaa400>
- Aniaku, S. E., Collins, O. C., & Onah, I. S. (2023). Analysis and optimal control measures of a typhoid fever mathematical model for two socio-economic populations. *Mathematics*, 11(23), 4722. <https://doi.org/10.3390/math11234722>

- Fiadufe, F. (2021). Mathematical modelling of typhoid fever disease incorporating delay caused by false negative diagnosis (MPhil thesis). University of Cape Coast, Ghana.
- Idowu, O. K., Erinle-Ibrahim, L. M., Agbomola, J. O., & Olawale-Shosanya, S. O. (2025). Effect of Environmental Precaution on the Transmission of Typhoid Fever: A Mathematical Modelling Approach. *E-Journal of Science and Mathematical Technology*, 12(1), 10. <https://doi.org/10.37134/ejsmt.vol12.1.10.2025>
- Khadija, O., Khassal, S., Khajji, B., & Balatif, O. (2026). Mathematical modeling and optimal control strategies of the typhoid transmission with cost-effectiveness analysis. *Iranian Journal of Numerical Analysis & Optimization*, 16(1). <https://doi.org/10.22067/ijnao.2025.94317.1676>
- Lawal, F., Yusuf, T., & Abidemi, A. (2024). On mathematical modelling of optimal control of typhoid fever with efficiency analysis. *Journal of the Nigerian Society of Physical Sciences*, 2057. <https://doi.org/10.46481/jnsps.2024.2057>
- Lawal, F. O., Yusuf, T. T., Abidemi, A., & Olotu, O. (2024). A non-linear mathematical model for typhoid fever transmission dynamics with medically hygienic compartment. *Modeling Earth Systems and Environment*. <https://doi.org/10.1007/s40808-024-02111-2>
- Madubueze, C. E., Gweryina, R. I., & Tijani, K. A. (2021). A dynamic model of typhoid fever with optimal control analysis. *Ratio Mathematica*, 41, 255.
- Nana-Kyere, S., Asamoah, J. K. K., Ankamah, J. D., Okyere, E., Seidu, B., Kwarteng, D., Ayetey, E. L., & Odum, J. K. (2025). Mathematical Modeling and Cost-Effectiveness Analysis of an SeEeIeRe Typhoid Fever Model. *Journal of Mathematics*, 1212057. <https://doi.org/10.1155/jom/1212057>
- Nyerere, N., Mpeshe, S. C., Ainea, N., Ayoade, A. A., & Mgandu, F. A. (2024). Global sensitivity analysis and optimal control of typhoid fever transmission dynamics. *Mathematical Modelling and Analysis*, 29(1), 141-160. <https://doi.org/10.3846/mma.2024.17859>
- Okolo, P., & Abu, O. (2020). On optimal control and cost-effectiveness analysis for typhoid fever model. *Fudma Journal of Sciences*, 4(3), 437-445. <https://doi.org/10.33003/fjs-2020-0403-258>
- Peter, O. J., Ibrahim, M. O., Edogbanya, H. O., Oguntolu, F. A., Oshinubi, K., Ibrahim, A. A., ... & Lawal, J. O. (2021). Direct and indirect transmission of typhoid fever model with optimal control. *Results in Physics*, 27, 104463. <https://doi.org/10.1016/j.rinp.2021.104463>
- Pitzer, V. E., et al. (2014). Mathematical modeling of typhoid fever. *Clinical Infectious Diseases*, 58(Suppl. 1), S4-S11. <https://doi.org/10.1093/cid/cit679>
- Raina, A. A., Ali, S., Kalra, P., & Modibbo, U. M. (2026). Adaptive Neuro-Fuzzy Inference System for Transmission Dynamics of HIV with an SEIRS Epidemic Model. *New Mathematics and Natural Computation*, 22(04), 1303-1325. <https://doi.org/10.1142/S1793005726500651>
- Sharma, L., & Kumar, R. (2026). Transmission dynamics of typhoid fever with nonlinear incidence rate and saturated treatment. *International Journal of Dynamics and Control*, 14(1), 6. <https://doi.org/10.1007/s40435-025-01953-7>

- Tijani, K. A., Madubueze, C. E., & Gweryina, R. I. (2024). Modelling typhoid fever transmission with treatment relapse response: Optimal control and cost-effectiveness analysis. *Mathematical Models and Computer Simulations*, 16(3), 457-485. <https://doi.org/10.1134/S2070048224700169>
- Tilahun, G. T., Makinde, O. D., & Malonza, D. (2017). Modelling and optimal control of typhoid fever disease with cost-effective strategies. *Computational and Mathematical Methods in Medicine*, 2017, 2324518. <https://doi.org/10.1155/2017/2324518>
- Tumwekwatse, O., Nanfuka, M., & Ariho, P. (2026). Modelling transmission dynamics of typhoid fever with vaccination, isolation and treatment of infected individuals. *International Journal of Mathematical Modelling and Numerical Optimisation*, 16(1), 82-107. <https://doi.org/10.1504/IJMMNO.2026.151104>
- Wameko, M., Koya, P., & Wodajo, A. (2020). Mathematical model for transmission dynamics of typhoid fever with optimal control strategies. *International Journal of Industrial Mathematics*, 12(3), 283-296.
- Watson, C. H., et al. (2017). A cross-sectional seroepidemiological survey of typhoid fever in Fiji. *PLoS Neglected Tropical Diseases*, 11(7), e0005786. <https://doi.org/10.1371/journal.pntd.0005568>



### Appendix A: Full Adjoint Equations and Optimality System

The complete adjoint system is:

$$\begin{aligned} \dot{\lambda}_1 &= \lambda_1(\gamma + \mu) - \lambda_2\gamma, \\ \dot{\lambda}_2 &= \lambda_2(\lambda + \mu + u_1) - \lambda_3(1 - \omega(1 - u_2))\lambda - \lambda_4\omega(1 - u_2)\lambda - \lambda_1u_1, \\ \dot{\lambda}_3 &= -A_1 + \frac{\partial \lambda}{\partial I} S[\lambda_2 - \lambda_3(1 - \omega(1 - u_2)) - \lambda_4\omega(1 - u_2)] + \lambda_3(\mu + \delta + \beta(1 + u_3)) - \lambda_5\beta(1 + u_3), \\ \dot{\lambda}_4 &= -A_2 + \frac{\partial \lambda}{\partial D} S[\lambda_2 - \lambda_3(1 - \omega(1 - u_2)) - \lambda_4\omega(1 - u_2)] + \lambda_4(\mu + \delta + \beta(1 + u_3)) - \lambda_5\beta(1 + u_3), \\ \dot{\lambda}_5 &= -\frac{\partial \lambda}{\partial T} S[\lambda_2 - \lambda_3(1 - \omega(1 - u_2)) - \lambda_4\omega(1 - u_2)] + \lambda_5\mu, \end{aligned}$$

with  $\lambda_j(T) = 0$ . The partial derivatives of  $\lambda$  are:

$$\frac{\partial \lambda}{\partial I} = \frac{\pi(1 - u_4)}{N} \theta_1, \quad \frac{\partial \lambda}{\partial D} = \frac{\pi(1 - u_4)}{N} \theta_2, \quad \frac{\partial \lambda}{\partial T} = -\frac{\pi(1 - u_4)}{N^2} (\theta_1 I + \theta_2 D).$$

The optimality system is solved by the forward-backward sweep algorithm described in (Lenhart & Workman, 2007).